PERGAMON

Journal of Structural Geology 21 (1999) 975–984

JOURNAL OF STRUCTURAL GEOLOGY

www.elsevier.nl/locate/jstrugeo

Are *S–C* structures, duplexes and conjugate shear zones different manifestations of the same scale-invariant phenomenon?

J. Hippertt

CNPq Researcher, Departamento de Geologia, Universidade Federal de Ouro Preto, 35400–000, Ouro Preto, MG, Brazil

Received 6 April 1998; accepted 2 February 1999

Abstract

By measuring *S* spacing, *C* spacing and the *S–C* angle (α) in deformed rocks, this paper investigates the geometry of previously published examples of *S–C* and *S–C*-like structures on a scale range between micrometres and several hundred kilometres. The results indicate that common *S–C* fabrics of thin-section, hand-specimen and outcrop scale, and conjugate fault/mylonite zones of map scale define a simple function $C_{spacing} = 2S_{spacing}$, which depicts a scale-invariant geometry over ten orders of magnitude. Logarithmic plots of cumulative frequency suggest that the *S–C* fractal set ($D = 0.13$) is restricted to the scale range between 600–800 μm and 1 km where genuine *S–C* structures, characterized by antithetic shear on the *S* planes, can be formed. Below 600–800 μm, grain scale processes seem to influence the development of *S–C* structures. Above the upper limit (1 km), only *S–C*-like structures with duplex kinematics (synthetic shear on *S* planes) occur. The *S–C* and *S–C–C′* fractals are envisaged as self-similar structures where the foliations work as both *S* or *C* planes, depending on which scale is considered.

1. Introduction

Scale-invariance within a specific scale range is a characteristic of some non-deterministic (chaotic) phenomena which are commonly referred to as *fractals* in the literature (Mandelbrot, 1982). Mathematically, a phenomenon is a fractal if the number of objects or events N with a characteristic size or value (length, area, volume, period of time, intensity, etc.) greater than L satisfies a power-law distribution $N \approx L^{-D}$, where D is the 'fractal dimension' of the data distribution. This fractal dimension reflects the relative abundance of small and big objects in the fractal set and characterizes the 'roughness' of the data distribution.

Geological phenomena are typically scale-invariant over a certain size range. That is why we must include a scale in any photograph of geological features, otherwise it is commonly impossible to know if the photo covers 10 cm or 10 km. Hence, it is not surprising that the concept of fractals has been applied with success to a number of geological processes and structures. The reader is referred to Turcotte (1992) and Barton and La Pointe (1995) for other geological applications of fractals. In this paper, an attempt is made to investigate the fractal nature of *S–C* structures, a common feature in anisotropic materials deformed in non-coaxial strain regimes in the ductile field, and their possible genetic connection with other structures of varied scales, such as duplexes and conjugate mylonite zones, which commonly show *S–C*-like geometries regardless of resulting from different mechanisms of formation.

2. *S–C* and *S–C*-like structures

An *S–C* fabric (Berthé et al., 1979) is a conjugate set of two foliations which were synchronously formed during a single, progressive, non-coaxial deformation event. The *C* planes are parallel to the bulk shear plane (defined by the shear zone boundaries), while the *S* planes are assumed to be parallel to the *XY* plane of finite strain within the 'low strain domains' between

E-mail address: hippertt@degeo.degeo.ufop.br (J. Hippertt)

0191-8141/99/$ - see front matter
PII: S0191-8141(99)00047-4

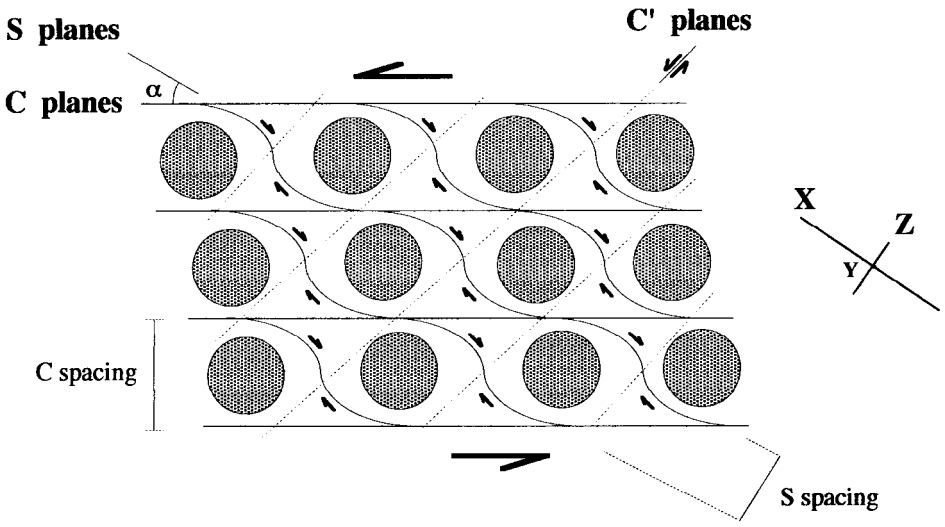

Fig. 1. Sketch illustrating the main characteristics of *S–C* fabrics viewed on the *XZ* plane of finite strain. The parameters *C* spacing, *S* spacing and *S–C* angle (α) which are treated in this paper are indicated. The circles represent relatively rigid objects (porphyroclasts).

two consecutive 'high strain domains' (*C* planes). Hence, the obliquity of the *S* planes relative to the *C* planes directly reflects the orientation of the finite strain ellipsoid, making *S–C* fabrics a reliable shear sense indicator (Simpson and Schmid, 1983; Hanmer and Passchier, 1991). Ideally, at low shear strain, the angle between *S* and *C* planes is close to 45°, decreasing with progressive strain due to rotation of the *S* planes in parallel with rotation of the finite strain ellipsoid during simple shear (Krohe, 1990). High strain mylonites commonly show subparallel sets of *S* and *C* planes. Eventually, a third set of planes (*C′* planes) may be formed at high angles to the maximum extension direction of finite strain in stretching shear zones (Passchier, 1991). Figure 1 summarizes the main characteristics of *S–C* fabrics.

Most strain in *S–C* fabrics is accommodated via synthetic shear on the *C* planes which act as the main fabric attractor (Passchier, 1997) during progressive simple shear. *C′* planes, when present, also accommodate synthetic shear. In contrast, a limited antithetic shear may operate on the *S* planes in consequence of rotation of the *XY* plane of finite strain (Krohe, 1990). This antithetic shear occurs if the pre-existing *S* planes are passively rotated in parallel with rotation of the *XY* plane of finite strain. This process is analogous to a card deck or set of dominos falling down, where antithetic shear occurs between the individual cards. Evidence for antithetic shear on *S* planes is more common in *S–C* structures of thin section and hand-specimen scales, appearing either as an offset of broken fragments (Hippertt, 1993), slip between basal planes of mica in mica-fish (Lister and Snoke, 1984) or asymmetric quartz *c*-axis fabrics (Krohe, 1990). Nevertheless, many *S–C* structures do not show any clear evidence of shear on the *S* planes, making obscure the meaning of *S* planes.

Depending on the material composition and rheology, different types of *S–C* fabrics are developed (Lister and Snoke, 1984). In mylonitic micaceous quartzites, for example, *S* and *C* planes may appear as a discontinuous planar fabric defined by the shape preferred orientation of isolated mica flakes disseminated in the quartzose matrix, not necessarily forming well-defined mica folia. This microstructure reflects a low degree of strain partitioning, as a consequence of a relatively homogeneous deformation on a thin-section scale via crystal–plastic processes in quartz and phyllosilicates. These *S–C* fabrics are not the focus of this paper.

Another type of *S–C* fabric typically develops in strongly anisotropic materials such as granitic mylonites which were sheared at low/medium metamorphic grade conditions, and correspond to the *S–C* fabrics originally defined by Berthé et al. (1979) and type-II *S–C* fabrics of Lister and Snoke (1984). In these rocks, the *S* and *C* planes generally appear as well-defined folia characterized by an enrichment in mica and quartz as well as grain size reduction. In these rheologically anisotropic materials, the *S* and *C* planes surround relatively rigid, mm- or cm-sized lenticular domains (microlithons) generally constituted by feldspar porphyroclasts. The *S* and *C* planes, therefore, should act as the main locus of movement in the deforming rock. Thus, if we analyse these *S–C* fabrics commonly observed in granitic mylonites on thin-section and hand-specimen scales (Fig. 2) in a purely kinematic point of view, we will see microzones of

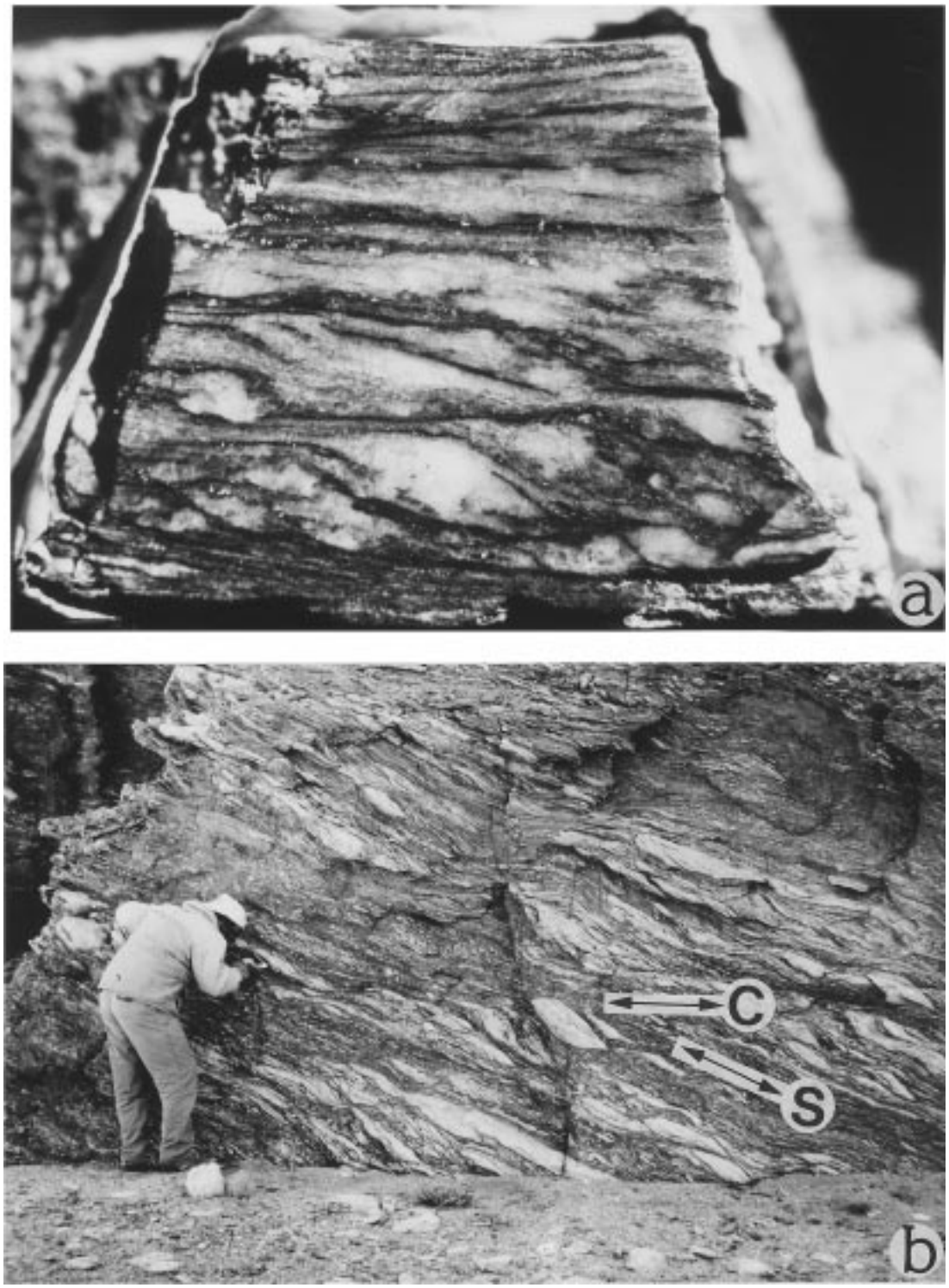

Fig. 2. *S–C* structures of different scales observed on the *XZ* plane of finite strain. (a) Typical hand-specimen scale *S–C* structure in a granitic mylonite (Moeda–Bonfim shear zone, southeastern Brazil). Note the decreasing angle between *S* and *C* towards the high strain domain on the top of photo. Width of view is 10 cm. (b) Outcrop scale *S–C* structure in a mylonitic gneiss from the eastern border of Puna, northwestern Argentina (photo by F. Hongn). The overall shear sense is sinistral in the two photos.

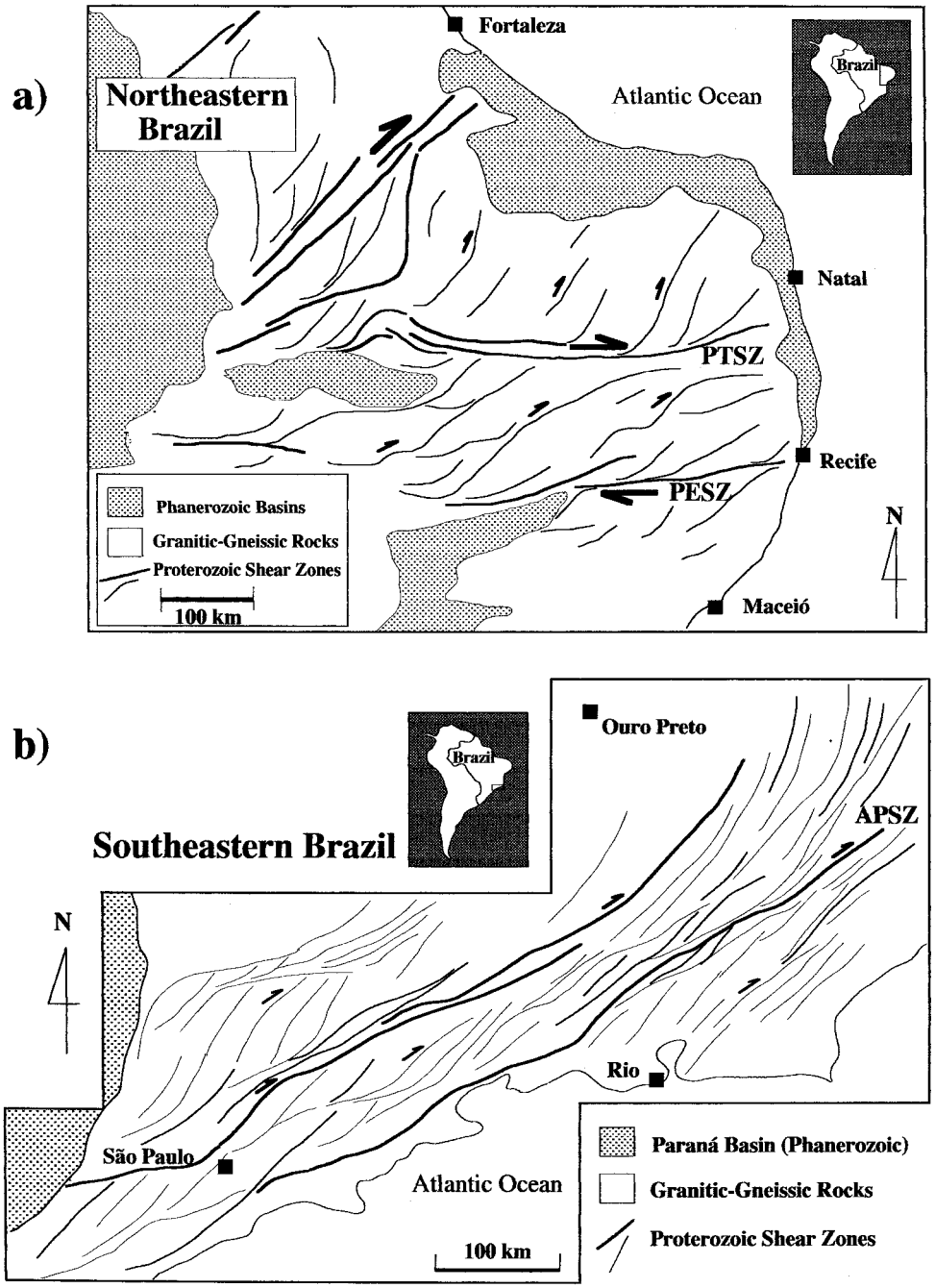

Fig. 3. Sets of shear zones with *S–C*-like geometry on map. (a) Strike-slip shear zones in the Borborema Province, northeastern Brazil (Davison et al., 1995). (b) Proterozoic strike-slip shear zones in the Mantiqueira Province, southeastern Brazil (modified from Ebert et al., 1996). Patos (PTSZ), Pernambuco (PESZ) and Além Paraíba (APSZ) shear zones are indicated.

movement (the *S* and *C* planes) separating relatively immobile lenticular domains (porphyroclasts). A similar situation occurs in conjugate sets of movement zones of outcrop and map scales with *S–C*-like geometries, which surround lenticular domains of relatively undeformed rocks (Fig. 3).

Encouraged by this initial qualitative analogy, I have performed a search of *S–C* fabrics and conjugate fault zones and mylonite zones with *S–C*-like geometries (thrust belts, duplex structures, etc.) previously published in the literature. I have covered the whole collection of the *Journal of Structural Geology*, the last five years of *Tectonophysics* and have also included the examples shown in three structural geology textbooks (Davis, 1984; Twiss and Moores, 1992; Passchier and Trouw, 1996). A total of 133 *S–C* and *S–C*-like struc-

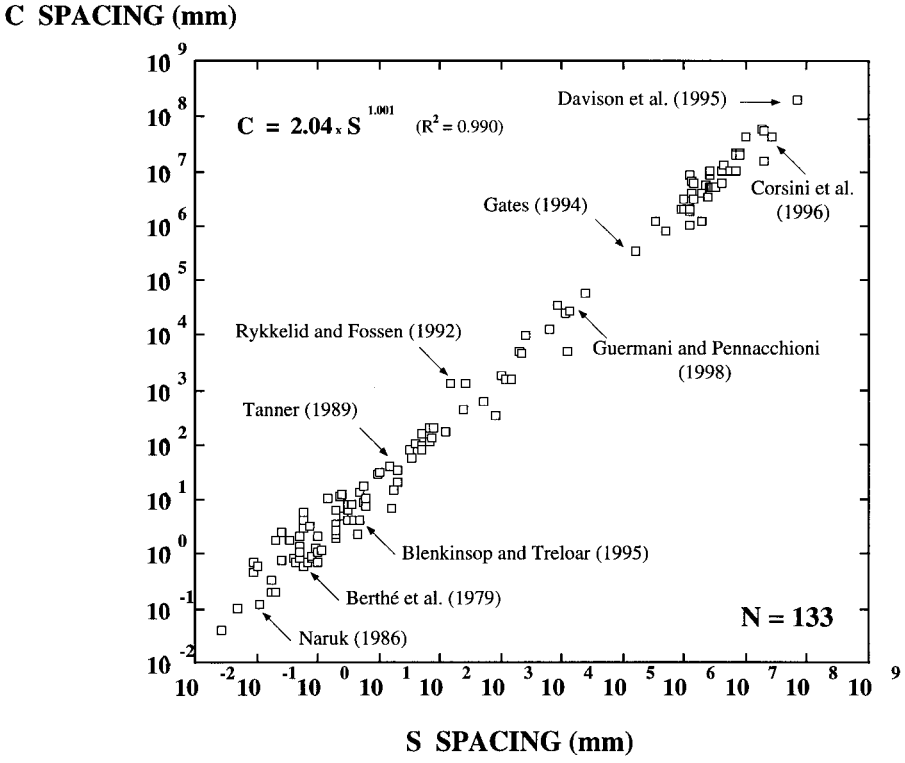

Fig. 4. Logarithmic plot of C spacing vs S spacing for published examples of S–C structures and fault/mylonite zones with S–C-like geometries. The data plot on a straight line defining a simple function close to $C = 2S$ with a goodness-of-fit $R > 99\%$.

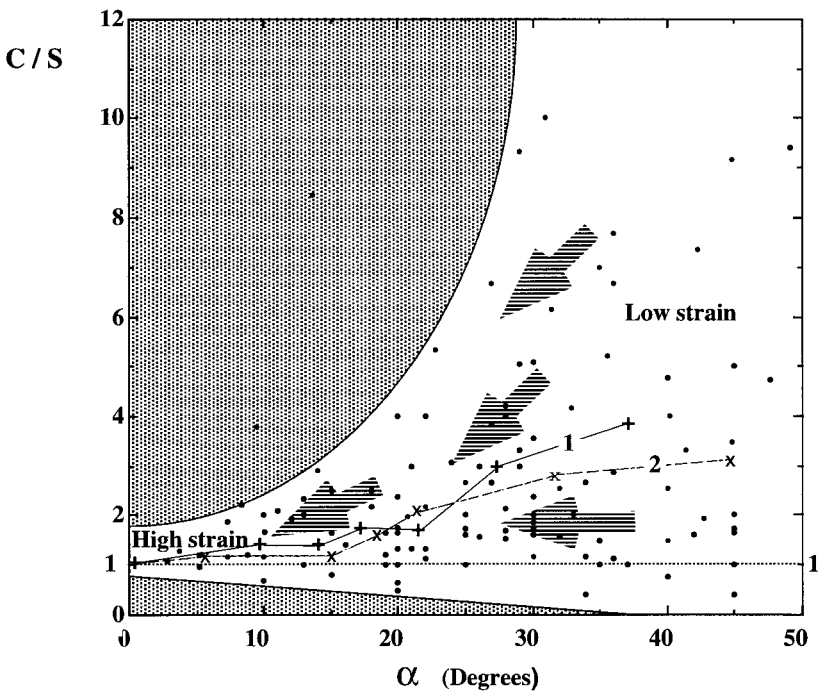

Fig. 5. Plot of C spacing/S spacing ratio (C/S) vs S–C angle (α) for all database. Trends 1 (Dutruge et al., 1995) and 2 (Moeda–Bonfim shear zone, southeastern Brazil) show the variation of C/S and α with progressive strain. Note that the C/S values converge to 1 at high strain levels (arrows).

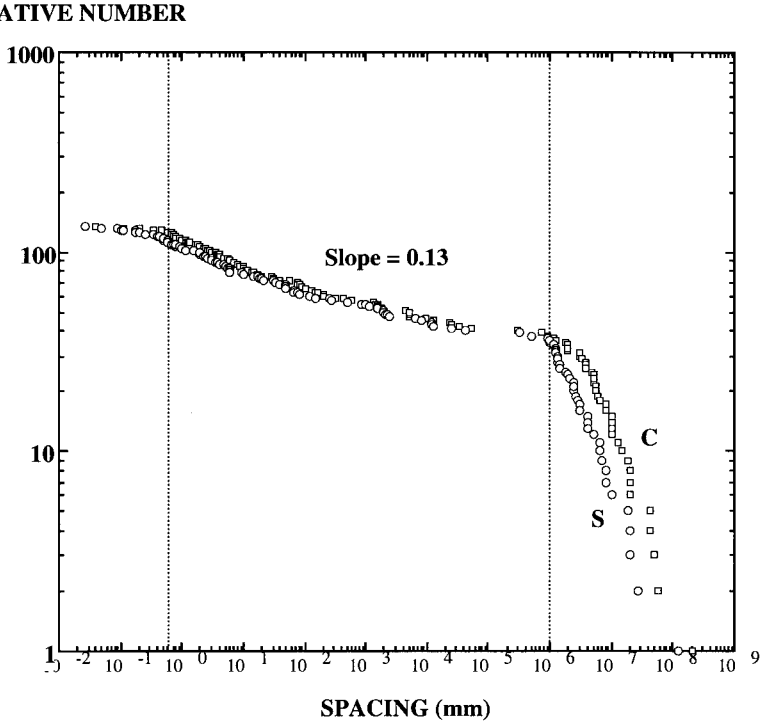

Fig. 6. Logarithmic plot of cumulative number for S spacing and C spacing. Smoothly curved central segments (slope = 0.13) appear between 600–800 μm and 1 km.

tures shown on the XZ plane of finite strain were found where there are well-defined S and C planes, an indication of shear sense on these planes and an accurate metric scale on the photo, sketch or map to permit measurements. This paper describes the statistical analysis carried out in this database.

3. Statistical analysis

I have measured the average spacing between adjacent S and C planes (S spacing and C spacing) in typical S–C fabrics as well as in conjugate movement zones of different scales which show a S–C-like geometry. Figure 4 shows a logarithmic plot of S spacing vs C spacing for the entire database. S–C fabrics of microscopic and hand-specimen scales and conjugate movement zones (faults and mylonite zones) of map scale plot on a same straight line according to a simple function $C_{\text{spacing}} = 2S_{\text{spacing}}$, with a goodness-of-fit $R > 99\%$. This simple function indicates that the relation between S spacing and C spacing is statistically constant along a scale range of ten orders of magnitude.

Although the whole database defines a simple function where the average C spacing/S spacing ratio (C/S) is around 2, the specific structures of any scale may show C/S values varying between 0.5 and 10. The range of C/S values becomes narrower with progressive strain and decreasing angle between the S and C planes (Fig. 5). At the highest strain levels, the C/S ratio converges to a final value of around 1, where the S and C planes would be theoretically parallel. To illustrate this trend, I have obtained C/S values for one published example of S–C structures shown at different degrees of progressive strain (Dutruge et al., 1995), and have also plotted the trend obtained in samples from the Moeda–Bonfim shear zone (Fig. 2a). These trends are shown in Fig. 5.

However, a scale-invariant geometry does not necessarily define a power-law data distribution which can only be confirmed if the data set defines a straight central segment on a logarithmic plot of cumulative frequency, where the negative slope of the power-law segment gives the fractal dimension (D) of the data population. The terminations of the straight segment may also indicate the lower and upper scale limits where the phenomenon behaves as a fractal. Geologically, the importance of identifying a power-law segment is to define the scale range where the phenomenon results from the operation of the same physical controls. The limits of the power-law segment, therefore, may represent scale limits where other processes begin to operate causing changes in the characteristics of the phenomenon.

Fig. 6 shows a logarithmic plot of cumulative frequency for both S spacing and C spacing of the entire database. The curves show the typical three segments

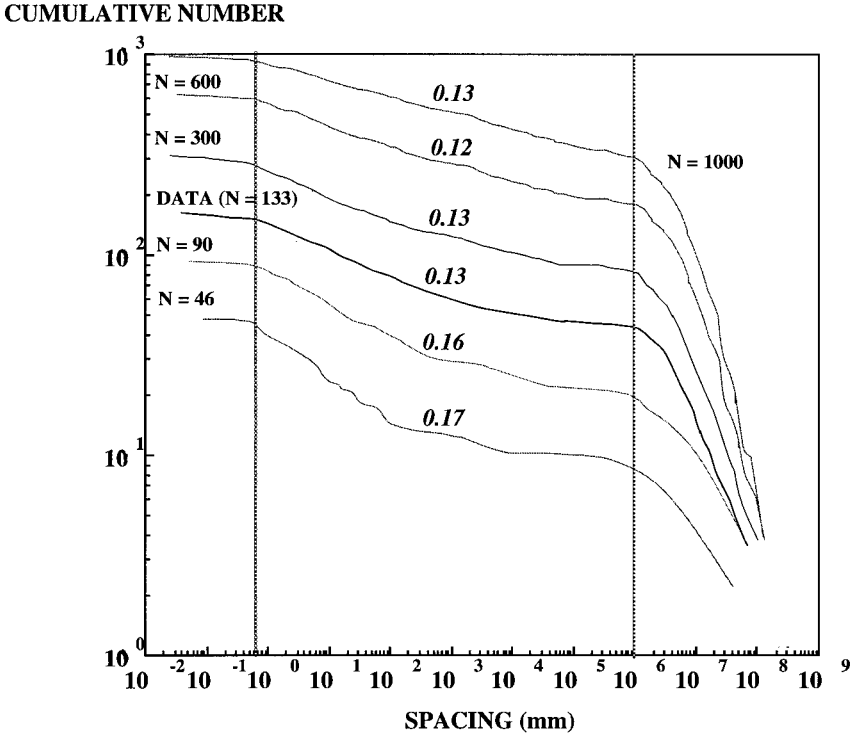

Fig. 7. Simulated curves produced through computer simulation of data with the same variance and clustering pattern as the database ($N = 133$). Note how the curvature becomes smoother with increasing N (see text).

present in power-law data distributions. The central segment extends over six orders of magnitude (from 600–800 μm to 1 km) with an average slope $D = 0.13$. Because this central segment is slightly curved, an attempt was made to test the statistical validity of the data set through plotting of simulated cumulative curves with lower and higher cumulative numbers (Fig. 7). The simulated curves with $N = 300$, 600 and 1000 were constructed by computer simulation of data following the same variance and clustering pattern of the real database. The simulated curves show progressively less curved segments with increasing N, with a nearly straight segment appearing with $N = 1000$. This simulation indicates that the smooth curvature of the central segment in the curves of Fig. 5 probably represents a sampling effect (e.g. Walsh et al., 1994), and not a deviation from the power-law distribution. Even with the changes in curvature with different N, the terminations of the central segment around 600–800 μm and 1 km are well-marked in all curves, reflecting the probable limits of the power-law distribution. Both the database and the simulated curves with $N > 100$ have central segments with similar slopes (0.12–0.13).

As commonly occurs in irregularly sampled databases, the logarithmic curves of S and C spacing (Fig. 6) show some gaps, the most noticeable one at the scale of one hundred metres. This may be a consequence of the lack of well-documented movement zones on this scale, as these structures are too large to be observed in an outcrop and too small to appear in most regional or local geological maps.

4. Discussion

The results indicate that common S–C fabrics of mm- and cm-scale and conjugate fault zones and mylonite zones with S–C-like geometries and average spacing in the order of several hundred metres fit within the same power-law data distribution with a fractal dimension $D = 0.13$, suggesting the operation of the same physical controls on their development. The lower limit of the power-law distribution (600–800 μm) probably represents the scale limit for influence of grain scale processes such as grain boundary migration, grain boundary sliding, pressure solution and reaction softening, which commonly contribute to the development of S–C fabrics of millimetre and micrometre scales (e.g. Gates, 1992). Indeed, below this size limit, typical S–C fabrics with well-defined mica folia are rare, and pervasive type-II S–C fabrics (Lister and Snoke, 1984) are more common. Similarly, the upper limit of the fractal set (1 km) may reflect the control exerted by compositional differences over large areas of a deforming rock on its rheology (e.g. variation of mica content in a granitic protolith), influencing the resulting geometry of conjugate movement zones of

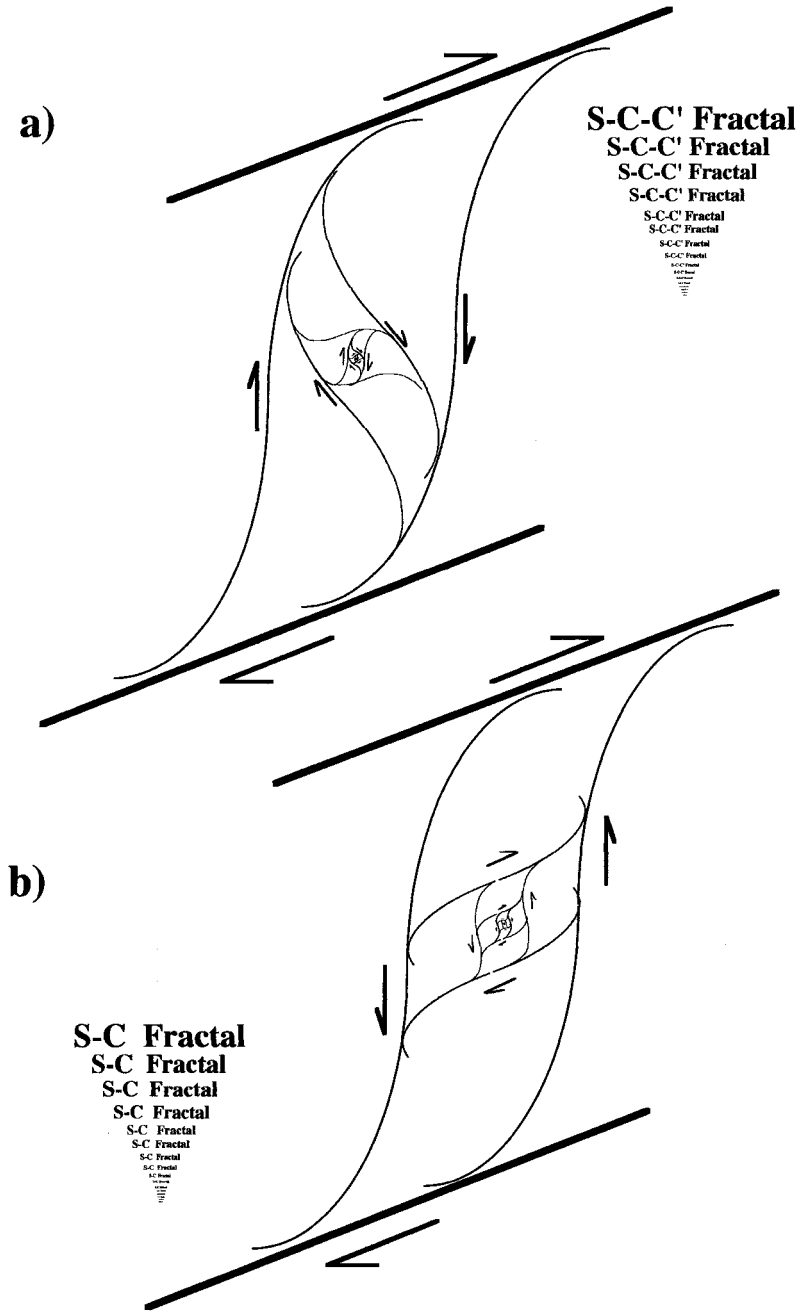

Fig. 8. Sketches showing the development of *S–C* structures in continuously decreasing scales. (a) Synthetic shear on the *S* planes leads to development of three planar fabrics whose orientation and kinematics are consistent with a *S–C–C′* geometry. (b) In contrast, the antithetic shear on the *S* planes which is a characteristic of genuine *S–C* structures, impedes the appearance of *C′* planes (Fig. 2b). Note how a particular movement plane can be envisaged either as *S* or *C* plane depending on which scale is considered.

map scale. This limit is suggested to represent the maximum dimension for occurrence of genuine *S–C* structures which are characterized by antithetic movements between *C* and *S* planes. Indeed, all the data plotting above this limit in Fig. 6, i.e. in the steeper termination of the curve, correspond to shear zones and duplex structures with *S–C*-like geometries, but with synthetic movements on the *S* and *C* planes. The relative sense of shear along the *S* planes is in fact the main difference between *S–C* structures and duplex structures with *S–C*-like geometries.

The results indicate that, although all *S–C* and *S–C*-like structures show a scale-invariant geometry over ten orders of magnitude (Fig. 4), the fractal set is restricted to the scale range between 600–800 μm and 1 km, where real *S–C* structures with respect to both

the geometry and the kinematics (i.e. with antithetic shear on S planes) can be formed. Figure 8 shows how the relative movements on the specific planes of a S–C structure leads to development of a fractal set, inducing the formation of secondary S–C structures in continuously decreasing scales. It is interesting to note how duplex kinematics (synthetic shear on the S planes) lead to development of three planar fabrics whose orientation and kinematics are consistent with a S–C–C' geometry (Fig. 8a). In contrast, an antithetic movement on the S planes impedes the appearance of C' planes (Fig. 8b).

The database includes structures with S and C planes making angles between 45 and 0°. The average C/S ratio for each angle decreases continuously from about 2.5–2 (S–C angle around 40–45°) to 1, when S and C are parallel. This trend is well-reflected in the two examples of progressive S–C fabrics shown in Fig. 5. In addition, the C/S values are spread on a wider range of values at lower degrees of finite strain. These relationships are interpreted to reflect a more prominent nucleation of C planes (hence, decreasing the C/S ratio) at low degrees of finite strain. In contrast, at the high strain levels ($\alpha<15°$), where a pervasive set of C planes is already developed, deformation can be efficiently accommodated by passive rotation of the S planes towards the C planes, without significant generation of new C planes. As a consequence, the C/S spacing ratio decreases with a lower rate. This explains the kinks around 15–20° in the two trends plotted in Fig. 5.

In summary, the results show that different deformational processes can produce identical S–C geometries on a wide range of sizes. The S–C geometry is, therefore, suggested to represent an ideal layout for operation of different heterogeneous strain mechanisms (such as foliation development, formation of anastomosing sets of faults and shear zones, duplexes, etc.). In this layout, the planes S, C and C' are a suitable strain pathway where larger scale homogeneous deformation can be resolved into local finite strain components, on a wide range of sizes. In contrast, the magnitude and shear sense of the specific movements on the S, C and C' planes are diagnostic for each particular mechanism, whose operation is clearly scale-dependent and controlled by factors such as the rock rheology and the overall kinematic framework.

5. Conclusions

In answering the question 'Are S–C structures, duplexes and conjugate shear zones different manifestations of the same scale-invariant phenomenon?', this paper has reached four main conclusions:

1. Common S–C fabrics of thin-section and hand-specimen scale fit the same simple function, $C_{spacing} = 2S_{spacing}$, as outcrop and map scale fault zones and mylonite zones with S–C-like geometries. This defines a scale-invariant geometry over ten orders of magnitude.
2. The results indicate that although S–C and S–C-like structures show a scale-invariant geometry, the power-law distribution (slope = 0.13) is restricted to the scale range between 600–800 μm and 1 km, where genuine S–C structures with respect to both the geometry and the kinematics (i.e. with antithetic shear on S planes) can be formed.
3. The lower limit of the fractal set is interpreted to represent the beginning of influence of grain scale processes in the development of S–C fabrics. The upper limit may represent a size limit beyond which only S–C-like structures with a typical duplex kinematics (synthetic movements on the S and C planes) can be formed.
4. Most of the S and C planes present in a S–C structure of any size were probably formed at low/intermediate strain levels (S–C angles between 45 and 25°). At the high strain levels, strain is more efficiently accommodated by passive rotation of the S planes towards the C planes, without significant generation of new planes.

Acknowledgements

Financial support for this research was provided by FAPEMIG (process CEX 117/95) and the Brazilian National Research Council (CNPq, process 52.3688/96-2). I would like to thank E. Tohver and A. Massucatto for fruitful discussions, and F. Hongn for providing the photograph shown in Fig. 2(b). A special thanks is given to Wanusa Araujo, who patiently searched the literature looking for S–C and S–C-like structures. Constructive journal reviews were made by J. Behrmann and J. Watterson.

References

Barton, C., La Pointe, P., 1995. Fractals in the Earth Sciences. Plenum Press, New York.

Berthé, D., Choukroune, P., Jegouzo, P., 1979. Orthogneiss, mylonite and non-coaxial deformation of granites: the example of the South Armoricain shear zone. Journal of Structural Geology 1, 31–42.

Davis, G., 1984. Structural Geology of Rocks and Regions. John Wiley, New York.

Davison, I., McCarthy, M., Powell, D., Torres, H., Santos, C., 1995. Laminar flow in shear zones: the Pernambuco Shear Zone, NE-Brazil. Journal of Structural Geology 17, 149–161.

Dutruge, G., Burg, J.-P., Lapierre, J., Vigneresse, J.L., 1995. Shear strain analysis and periodicity within shear gradients of metagranite shear zones. Journal of Structural Geology 17, 819–830.

Ebert, H., Chemale Jr, F., Babinski, M., Artur, A., Van Schmus, W., 1996. Tectonic setting and U/Pb zircon dating of the plutonic Socorro complex in the transpressive Rio Paraíba do Sul shear belt, SE Brazil. Tectonics 15, 688–699.

Gates, A., 1992. Domainal failure of serpentinite in shear zones, State-Line mafic complex, Pennsylvania, U.S.A. Journal of Structural Geology 14, 19–28.

Guermani, A., Pennachioni, G., 1998. Brittle precursors of plastic deformation in a granite: an example from the Mont Blanc massif (Helvetic, western Alps). Journal of Structural Geology 20, 135–148.

Hanmer, S., Passchier, C., 1991. Shear sense indicators: a review. Geological Survey of Canada, Paper 90, 1–71.

Hippertt, J., 1993. 'V'-pull-apart microstructures: a new Shear-sense indicator. Journal of Structural Geology 15, 1393–1403.

Krohe, A., 1990. Local variations in quartz *c*-axis orientations in non-coaxial regimes and their significance for the mechanics of *S–C* fabrics. Journal of Structural Geology 12, 995–1004.

Lister, G., Snoke, A., 1984. *S–C* mylonites. Journal of Structural Geology 6, 617–638.

Mandelbrot, B.B., 1982. The Fractal Geometry of Nature. W.H. Freeman, San Francisco.

Naruk, J., 1986. Strain and displacement across the Pinaleño Mountains shear zone, Arizona, U.S.A. Journal of Structural Geology 8, 35–46.

Passchier, C., 1991. Geometric constraints on the development of shear bands in rocks. Geologie en Mijnbouw 70, 203–211.

Passchier, C., 1997. The fabric attractor. Journal of Structural Geology 19, 113–127.

Passchier, C., Trouw, R., 1996. Microtectonics. Springer-Verlag, Berlin.

Rykkelid, E., Fossen, H., 1992. Composite fabrics in mid-crustal gneisses: observations from the Øygarden Complex, West Norway Caledonides. Journal of Structural Geology 14, 1–10.

Simpson, C., Schmid, S., 1983. An evaluation of criteria to determine the sense of movement in sheared rocks. Geological Society of America Bulletin 94, 1281–1288.

Tanner, P., 1989. The flexural slip mechanism. Journal of Structural Geology 11, 635–655.

Turcotte, D.L., 1992. Fractals and Chaos in Geology and Geophysics. Cambridge University Press, Cambridge.

Twiss, R., Moores, E., 1992. Structural Geology. W.H. Freeman, New York.

Walsh, J., Watterson, J., Yielding, G., 1994. Determination and interpretation of fault size populations: procedure and problems. In: Buller, A.T., et al. (Eds.), North Sea Oil and Gas Reservoirs III. Norwegian Institute of Technology, pp. 141–155.